Methods

Reagents

Human liver microsomes of EM (*1/*1, pooled lot from more than 20 subjects) and PM (*4/*4) were purchased from Gentest (Massachusetts, USA). Human liver *10/*10 microsomes from three Chinese subjects were purchased from RILD (Shianghai, China). Tamoxifen, beta-nicotinamide adenine dinucleotide phosphate sodium salt (NADPH), D-glucose 6-phosphate disodium salt hydrate (G6P), and glucose 6-phosphate dehydrogenase (G6P-DH) were purchased from Sigma (Missouri, USA). 4-Hydroxytamoxifen and *N*-desmethyltamoxifen were purchased from Toronto Research Chemicals (Ontario, Canada). Other reagents of the highest grade available were used. EDX was synthesized from 4-hydroxytamoxifen according to the method of Pelander *et al.* (9).

Incubation of human liver microsome

Microsome incubation was performed to metabolize NDM to EDX. The incubation was initiated by an addition of 0.5 mM NADPH into 10 mL glass tubes with glass lids pooled with 0.1 mM EDTA, 2 mM G6P, 4 mM $MgCl_2$, 1 U/mL G6P-DH, 30 μM NDM, and microsome (0.25-1.0 mg protein/mL). The final volume was 0.3 mL. The glass tubes were incubated for 0 or 10 min at 37°C. The incubation was terminated by an addition of 0.1 mL ice-cold Glycine/Na buffer (pH 11.3). An internal standard (100 nM propranolol in DMSO) and 3 mL of hexane : isopropanol (95:5) were added, shaken for 30 min, and then centrifuged at 3000*g* for 5 min. The upper phase was transferred to a 10 mL glass tube, evaporated to dryness, and resolved in 0.1 mL of the HPLC mobile phase described below.

Quantification of EDX

EDX was quantified by an HPLC method with online derivatization to a fluorescent compound by a photoreactor according to a method by Lee *et al.* (10) with some modifications. The HPLC system was composed of a controller (SCL-10A), pumps (LC-10AD), an auto injector (SIL-10AXL), a degasser (DGU-4A), a column oven (CTO-10A), a fluorometric detector (RF-10A), and an integrator (C-R7Aplus), from Shimadzu (Kyoto, Japan). A UV photoreactor (tube length 5 m, S-3900, Soma Optics,

Tokyo, Japan) was attached prior to the fluorometric detector for postcolumn derivation. The chromatographic separation was carried out on a CN column (YMC-Pack CN, 0.005 mm, 4.6 x 250 mm, YMC, Kyoto, Japan) connecting with a CN guard column (YMC, Kyoto, Japan) by using a mobile phase composed of 0.1 M formic acid (pH 3.0) and acetonitrile (70.5:29.5, v/v) at the flow rate of 1.0 mL/min. The column temperature was set at 40 °C. An aliquot (80 μL) of the sample was injected into the HPLC and the fluorescence of photoreacted derivatives in the effluents was detected at EM 256 nm, EX 380 nm. The detection limit of EDX was 2 nM, and the linearity was confirmed up to 500 nM.

Prediction of the plasma concentration of EDX in CYP2D6*10 carriers

The ratios of the steady-state plasma concentration of EDX in CYP2D6*10/*10 and *1/*10 carriers to that in *1/*1 carriers were predicted by the following two steps. In the first step, the contribution of CYP2D6 in the overall oxidative metabolism of TAM to EDX by various CYPs was estimated from *in vitro* kinetic parameters of the TAM biotransformation in human liver microsome reported by Desta *et al.* (11). The fraction of Substrate A to be transformed to Metabolite B ($F_{A\rightarrow B}$) was estimated by intrinsic clearances (CL_{int}), which were calculated by V_{max}/K_m reported in the literature as follows:

$$F_{A\rightarrow B} = \frac{CL_{int,A\rightarrow B}}{CL_{int,A\rightarrow B} + \sum CL_{int,A\rightarrow Others}} \qquad \text{Eq.1}$$

We used the mean value of the kinetic parameters reported by Desta *et al.* (11), with an exception for $F_{NDM\rightarrow EDX}$. For the determination of $F_{NDM\rightarrow EDX}$, we omitted the value of the lowest CYP2D6 metabolizing activity which may be collected from PM (11). The fractions to EDX from TAM *via* NDM and that *via* 4-OH were calculated by the following equations, respectively:

$$F_{TAM\rightarrow EDX,NDM} = F_{TAM\rightarrow NDM} \times F_{NDM\rightarrow EDX} \qquad \text{Eq.2}$$

$$F_{TAM\rightarrow EDX,4\text{-}OH} = F_{TAM\rightarrow 4\text{-}OH} \times F_{4\text{-}OH\rightarrow EDX} \qquad \text{Eq.3}$$

The contribution of CYP2D6 to the overall process from TAM to EDX ($F_{TAM\rightarrow EDX,}$

$_{2D6}$) was estimated by the following equation considering that the biotransformation from NDM to EDX is exclusively mediated by CYP2D6 (2).

$$F_{TAM \rightarrow EDX,2D6} = \frac{F_{TAM \rightarrow EDX,NDM}}{F_{TAM \rightarrow EDX,NDM} + F_{TAM \rightarrow EDX,4-OH}} \quad \text{Eq.4}$$

In the second step, we predicted the ratios of the steady-state plasma concentration of EDX in CYP2D6*10/*10, *1/*10, PM (assuming *4/*4), and IM (assuming *1/*4) subjects *versus* *1/*1 subjects (R) according to the following equations:

$$R_{*10/*10} = 1 - F_{TAM \rightarrow EDX,2D6} \times (1 - ratio_{*10}) \quad \text{Eq. 5}$$

$$R_{*1/*10} = 1 - F_{TAM \rightarrow EDX,2D6} \times (1 - ratio_{*10}) \times 1/2 \quad \text{Eq. 6}$$

$$R_{PM} = 1 - F_{TAM \rightarrow EDX,2D6} \quad \text{Eq. 7}$$

$$R_{IM} = 1 - F_{TAM \rightarrow EDX,2D6} \times 1/2 \quad \text{Eq. 8}$$

In these equations, "$ratio_{*10}$" refers to *in vitro* EDX formation ratio from NDM by *10/*10 liver microsome divided by that by wild type microsome, which were obtained in the present study.

The steady state plasma concentrations of TAM, NDM, 4OH and EDX in *1/*1 subjects were obtained from results of the clinical research by Jin *et al.* (5). We assumed that the concentrations of TAM, NDM and 4-OH were not altered in *10/*10, *1/*10, PM, and IM subjects. Relative plasma antiestrogenic potencies in *10/*10, *1/*10, PM, and IM subjects during the TAM therapy were calculated as the sum of products of the estimated plasma concentrations of TAM, NDM, 4-OH and EDX with relative antiestrogenic activities as 1 for TAM and NDM, and 100 for 4-OH and EDX (1, 2).

Results and Discussion

The conversion of TAM to EDX consists of several biological transformation processes mediated by cytochrome P450 enzymes, and the overall process is so slow

that the direct measurement *in vitro* is unpractical (Fig. 1). The process includes two pathways; the major pathway is *via* NDM and the minor one is *via* 4-OH (Fig. 1).

It has been reported that CYP2D6 exclusively mediates the transformation of NDM to EDX, while some contribution to a transformation of TAM to 4-OH was also suggested (Fig. 1, Ref. 2). The transformation from TAM to NDM and that from 4-OH to EDX are mediated by CYP3A4 and 3A5 (Fig. 1). In the present study, we hypothesized that the NDM pathway should be abolished completely in the absence of CYP2D6, whereas the contribution of CYP2D6 to the 4-OH pathway is minimal. This hypothesis is supported by the fact that the plasma concentration of EDX decreased markedly in PM of CYP2D6 whereas the concentration of 4-OH was not altered (5). Based on these considerations, we focused our efforts to the conversion of NDM to EDX, in order to evaluate the contribution of CYP2D6 in generation of EDX.

In our experiments, metabolizing velocities for the formation of EDX from NDM were 6.3±2.0 and 26.8 (pmol/min/mg protein, mean±SD) in liver microsomes from CYP2D6*10/*10 carriers (n = 3) and EM (a pooled lot), respectively (Fig. 2). EDX was not detectable by incubating NDM with the human liver microsome from PM. These results suggest that the metabolism to EDX from NDM is exclusively mediated by CYP2D6 and its activity in *10/*10 carriers is reduced to 23.4% of EM. In general, together with *1/*4 and *1/*5 carriers, *10/*10 carriers are classified as IM. However, by considering the marked decrease in the formation of EDX in *10/*10 microsome, there emerges a need not only in PM but also in *10/*10 carriers to inquire for plasma EDX concentration and clinical outcome of TAM therapy.

From the reanalysis of *in vitro* data reported in Ref. 11, it was estimated that 82% of TAM is metabolized to NDM in the liver and then 17% of NDM is followed by the further transformation to EDX (Fig. 1). In parallel, 6.1% of TAM is metabolized to 4-OH and then 48% of 4-OH is followed by a transformation to EDX (Fig. 1). Consequently, the respective contribution ratios of the NDM and the 4-OH pathways were estimated to be 83 and 17% of the overall generation of EDX.

The result of the prediction of plasma EDX concentrations utilizing *in vitro* and our present results are summarized in Table 1. Considering our results, EDX formation *via* NDM would be reduced in *10/*10 and *1/*10 subjects, and total EDX formation were predicted to be 36% and 68% of control, respectively (Table 1). In the same way, in the PM (inactive variants) and IM (hetero-carrier of inactive variants), the total EDX formation were predicted to be 17% and 59% of control, respectively

(Table 1). Concerning the human *in vivo* results, the observed plasma EDX concentration in PM and IM patients taking TAM were reported to be 26% and 55% of EM, respectively (Table 1 and Ref. 5). If we consider the presence of additional metabolic pathway of 4-OH by SULT, it may be concluded that the clinical data of PM and IM may be satisfactorily predicted by the present analysis method. The present analysis predicted that the concentrations of EDX are in the order of PM < *10/*10 < IM < *1/*10 < EM.

We also simulated the relative plasma antiestrogenic potency during the TAM therapy, considering plasma concentrations and *in vitro* activities of TAM and its metabolites in PM, IM, *10/*10 and *1/*10 subjects (Fig. 3). The relative potency were calculated to decrease to 49 and 74% in *10/*10 and *1/*10 subjects, and 34 and 67% in PM and IM, respectively (Fig. 3). Although these results need to be quantitatively compared with the actual outcomes of TAM therapy, we could provide the basic information for the individualized therapy of TAM.

Considering the high frequency of *10 allele in the East Asian population, it could be predicted that one fifth of this population, who are *10/*10 carriers, may not be receiving enough benefit from TAM therapy in spite of the long term therapy. The results of the present study suggest that the individualized TAM dosage according to CYP2D6 genotype would be clinically beneficial not only for Caucasians but also for East Asian patients.

In conclusion, our microsome incubation results showed that CYP2D6*10/*10 carriers would have 23% of the metabolizing activity from TAM to EDX compared to EM. Together with the reported data, we estimated that the antiestrogenic potency of TAM therapy would be in the order of PM < *10/*10 < IM < *1/*10 < EM. Considering the high frequency of *10 allele in East Asians, individualized TAM therapy would be clinically beneficial for East Asian patients having CYP2D6 variants with decreasing activity.

References

1. Johnson, M.D., Zuo, H., Lee, K.H., Trebley, J.P., Rae, J.M., Weatherman, R.V., Desta, Z., Flockhart, D.A., and Skaar, T.C.: Pharmacological characterization of 4-hydroxy-N-desmethyl tamoxifen, a novel active metabolite of tamoxifen. *Breast Cancer Res. Treat.*, **85**:151-9 (2004).
2. Stearns, V., Johnson, M.D., Rae, J.M., Morocho, A., Novielli, A., Bhargava, P., Hayes, D.F., Desta, Z., and Flockhart, D.A: Active tamoxifen metabolite plasma concentrations

after coadministration of tamoxifen and the selective serotonin reuptake inhibitor paroxetine. *J. Natl. Cancer Inst.*, **95**:1758-64 (2003).

3. Kim, M.K., Cho, J.Y., Lim, H.S., Hong, K.S., Chung, J.Y., Bae, K.S., Oh, D.S., Shin, S.G., Lee, S.H., Lee, D.H., Min, B., and Jang, I.J.: Effect of the CYP2D6 genotype on the pharmacokinetics of tropisetron in healthy Korean subjects. *Eur. J. Clin. Pharmacol.*, **59**:111-6 (2003).
4. Yu, A., Kneller, B.M., Rettie, A.E., and Haining, R.L.: Expression, purification, biochemical characterization, and comparative function of human cytochrome P450 2D6.1, 2D6.2, 2D6.10, and 2D6.17 allelic isoforms. *J. Pharmacol. Exp. Ther.*, **303**:1291-300 (2002).
5. Jin, Y., Desta, Z., Stearns, V., Ward, B., Ho, H., Lee, K.H., Skaar, T., Storniolo, A.M., Li, L., Araba, A., Blanchard, R., Nguyen, A., Ullmer, L., Hayden, J., Lemler, S., Weinshilboum, R.M., Rae, J.M., Hayes, D.F., and Flockhart, D.A.: CYP2D6 genotype, antidepressant use, and tamoxifen metabolism during adjuvant breast cancer treatment. *J. Natl. Cancer Inst.*, **97**:30-9 (2005).
6. Goetz, M.P., Rae, J.M., Suman, V.J., Safgren, S.L., Ames, M.M., Visscher, D.W., Reynolds, C., Couch, F.J., Lingle, W.L., Flockhart, D.A., Desta, Z., Perez, E.A., and Ingle, J.N.: Pharmacogenetics of tamoxifen biotransformation is associated with clinical outcomes of efficacy and hot flashes. *J. Clin. Oncol.*, **23**:9312-8 (2005).
7. Tateishi, T., Chida, M., Ariyoshi, N., Mizorogi, Y., Kamataki, T., and Kobayashi, S.: Analysis of the CYP2D6 gene in relation to dextromethorphan O-demethylation capacity in a Japanese population. *Clin. Pharmacol. Ther.*, **65**:570-5 (1999).
8. Johansson, I., Oscarson, M., Yue, Q.Y., Bertilsson, L., Sjoqvist, F., and Ingelman-Sundberg, M.: Genetic analysis of the Chinese cytochrome P4502D locus: characterization of variant CYP2D6 genes present in subjects with diminished capacity for debrisoquine hydroxylation. *Mol. Pharmacol.*, **46**:452-9 (1994).
9. Pelander, A., Ojanperä, I., and Hase, T. A.: Preparation of N-demethylated drug metabolites for analytical purposes using 1-chloroethyl chloroformate. *Forensic Science International.*, **85**:193-198 (1997).
10. Lee, K.H., Ward, B.A., Desta, Z., Flockhart, D.A., and Jones, D.R.: Quantification of tamoxifen and three metabolites in plasma by high-performance liquid chromatography with fluorescence detection: application to a clinical trial. *J. Chromatogr. B Analyt. Technol. Biomed. Life Sci.*, **791**:245-53 (2003).
11. Desta, Z., Ward, B.A., Soukhova, N.V. and Flockhart, D.A.: Comprehensive evaluation of tamoxifen sequential biotransformation by the human cytochrome P450 system in vitro: prominent roles for CYP3A and CYP2D6. *J. Pharmacol. Exp. Ther.*, 310:1062-75

(2004).

12. Falany, J.L., Pilloff, D.E., Leyh, T.S., and Falany, C.N.: Sulfation of raloxifene and 4-hydroxytamoxifen by human cytosolic sulfotransferases. *Drug. Metab. Dispos.*, **34**:361-8 (2006).

Table 1 ····· Predicted EDX plasma concentrations in carriers of CYP2D6*10/*10, *1/*10、PM and IM genotypes during the TAM therapy.

Plasma concentrations of EDX were predicted for subjects with different genotypes of CYP2D6 gene. The prediction is based on the data shown in Fig. 2 and the metabolic scheme in Fig. 1. The results are given as the ratio to EM (*1/*1).

Genotype	Plasma concentration of EDX (ratio to EM)	
	Predicted	Observed[$1] (95% confidence interval)
*10/*10	0.36	-
*1/*10	0.68	-
PM[$2]	0.17	0.26 (0.14-0.37, n = 3)
IM[$3]	0.59	0.55 (0.43-0.68, n = 29)

$1: Data from Ref 5.

$1: Combinations of inactive alleles such as *4 and *5 are assumed.

$2: Genotype of *1/*4 or *1/*5 is assumed.

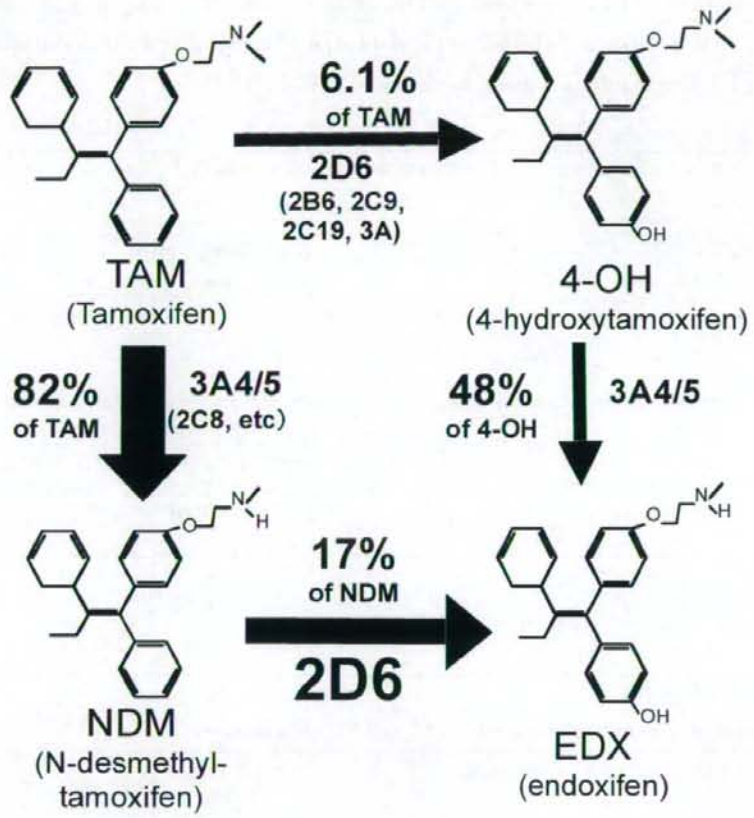

Fig. 1 ····· Collaboration of various CYPs in the metabolism of TAM to EDZ. Metabolic pathway of TAM to EDX is shown. The predicted values for the quantitative contribution of individual steps to the metabolism were calculated based on the literature data (11). See text for the detailed description.

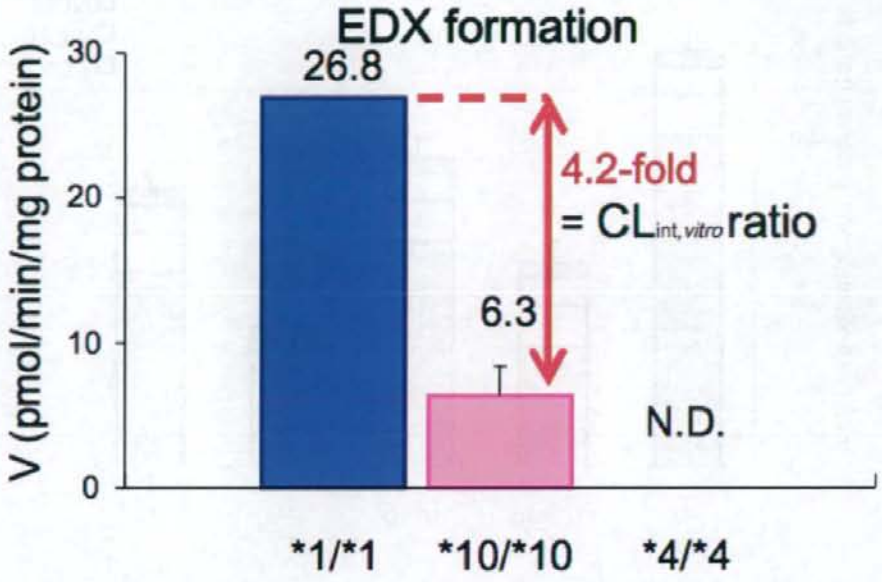

Fig. 2 ····· Metabolizing activities of EDX formation from NDM in human liver microsomes of different CYP2D6 genotypes. NDM (30 μM) was incubated with the human microsomes (0.25-1.0 mg protein / mL) with different genotypes of CYP2D6. For *1/*1, the microsome used was a pooled lot prepared from more than 20 subjects while *4/*4 microsome was prepared from one subject. For *10/*10 microsome, the mean ± SD of three individual lots are shown. All activities were determined by triplicate incubations. ND: not detected.

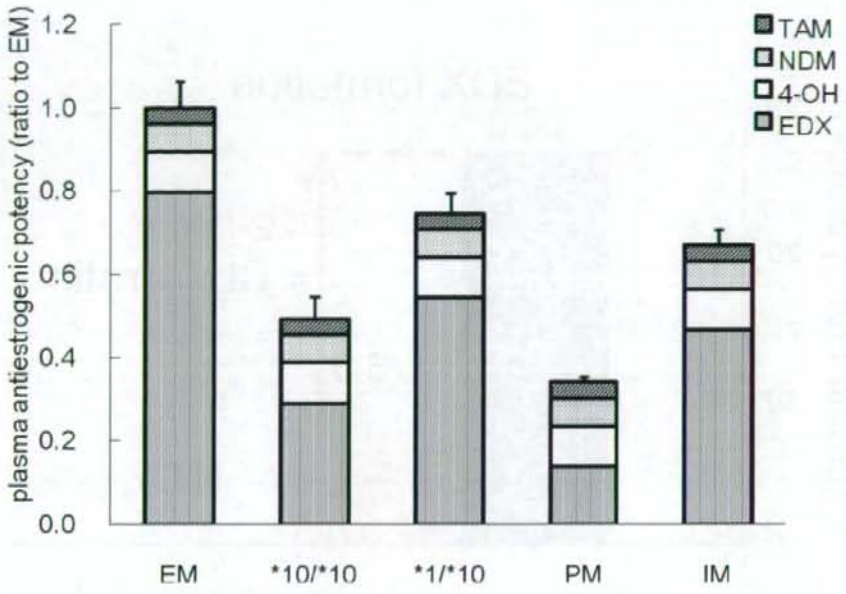

Fig. 3 ····· Predicted relative plasma antiestrogenic potency of TAM and its three metabolites in different CYP2D6 genotypes. Relative plasma antiestrogenic potency was calculated by multiplying the predicted plasma concentrations by the *in vitro* antiestrogenic activity of TAM and its subsequent metabolites. Data are presented as a ratio to EM. TAM: tamoxifen, NDM: N-desmethyltamoxifen, 4-OH: 4-hydroxytamoxifen, EDX: endoxifen

資料3.

General Framework for the Quantitative Prediction of CYP3A4-mediated Oral Drug Interactions Based on the AUC Increase by Coadministration of Standard Drugs

Yoshiyuki Ohno, Akihiro Hisaka, and Hiroshi Suzuki

Department of Pharmacy, The University of Tokyo Hospital, Faculty of Medicine, The University of Tokyo
Hongo 7-3-1, Bunkyo-ku, Tokyo 113-8655, Japan

(Clinical Pharmacokinetics, in press, 2007.)

ABSTRACT

Background:
Cytochrome P450 (CYP) 3A4 is the most prevalent metabolizing enzyme in the human liver and is also a target for various drug interactions of significant clinical concern. Even although there are numerous reports regarding drug interactions involving CYP3A4, it is far from easy to estimate all potential interactions, since too many drugs are metabolized by CYP3A4. For this reason, a comprehensive framework for the prediction of CYP3A4-mediated drug interactions would be of considerable clinical importance.

Objective:
The objective of this study is to provide a robust and practical method for the prediction of drug interactions mediated by CYP3A4 using minimal *in vivo* information from drug interaction studies, which are often carried out early in the course of drug development.

Data sources:
The analysis is based on 113 drug interaction studies reported in 78 published articles over the period 1983 to 2006. The articles were used if they contained sufficient information about drug interactions. Information on drug names, doses, and the magnitude of the increase in AUC were collected.

Methods:

The ratio of the contribution of CYP3A4 to oral clearance (CR_{3A4}) was calculated for 14 substrates (midazolam, alprazolam, buspirone, cerivastatin, atorvastatin, cyclosporin, felodipine, lovastatin, nifedipine, nisoldipine, simvastatin, triazolam, zolpidem, and telithromycin) based on plasma AUC increases observed in interaction studies with itraconazole or ketoconazole. Similarly, the time-averaged apparent inhibition ratio of CYP3A4 (IR_{3A4}) was calculated for 18 inhibitors (ketoconazole, voriconazole, itraconazole, telithromycin, clarithromycin, saquinavir, nefazodone, erythromycin, diltiazem, fluconazole, verapamil, cimetidine, ranitidine, roxithromycin, fluvoxamine, azithromycin, gatifloxacin, and fluoxetine) primarily based on AUC increases observed in interaction studies with midazolam. The increases in the AUC of a substrate associated with coadministration of an inhibitor were estimated using the equation $1 / (1 - CR_{3A4} \times IR_{3A4})$ based on pharmacokinetic considerations.

Results:

The proposed method enabled predictions of the AUC increase by interactions with any combination of these substrates and inhibitors (total 251 matches). In order to validate the reliability of the method, the AUC increases in an additional 60 studies were analyzed. The method successfully predicted AUC increases within 67-150% of the observed increase for 50 studies (83%), and within 50-200% for 57 studies (95%). Midazolam is the most reliable standard substrate for evaluation of the *in vivo* inhibition of CYP3A4. The present analysis suggests that simvastatin, lovastatin and buspirone can be used as alternatives. To evaluate the *in vivo* contribution of CYP3A4, ketoconazole or itraconazole is the selective inhibitor of choice.

Conclusion:

This method is applicable (1) to prioritize clinical trials to investigate drug interactions during the course of drug development, and (2) to predict the clinical significance of unknown drug interactions. If a drug interaction study is carefully designed using appropriate standard drugs, significant interactions involving CYP3A4 will not be missed. In addition, the extent of CYP3A4-mediated interactions between many other drugs can be predicted using the current method.

INTRODUCTION

Cytochrome P450 (CYP) 3A4 is the most prevalent CYP enzyme in the human liver. It accounts for approximately 30% of the total CYP enzymes in hepatic microsomes

and is involved in the metabolism of more than 50% of the drugs currently on the market.[1,2] CYP3A4 is also the target enzyme for a number of drug interactions of significant clinical concern. Drug interactions are one of the major sources of adverse events and some have actually led to drug withdrawals in the past.[3-5] Even although there are numerous reports on CYP3A4 drug interactions, it is far from easy to estimate all potential interactions, since too many drugs are metabolized by CYP3A4. For this reason, a comprehensive framework for the prediction of drug interactions would be of significant clinical importance. In addition, pharmaceutical companies are encouraged to carry out many *in vivo* drug interaction studies during the drug development process and the cost of these studies is increasing. Consequently, it is important to prioritize significant drug interactions to be confirmed as early as possible during the course of development. A reliable method for the prediction of CYP3A4 drug interactions would be advantageous in such circumstances.

A great deal of effort has already been devoted to establish a method for the accurate prediction of *in vivo* drug interactions using *in vitro* experimental data.[6-11] These predictions in principle rely on the $[I] / K_i$ ratio, that is a ratio of free concentration of the inhibitor at the interaction site to the *in vitro* inhibition constant. The results of these studies have increased our understanding of the mechanisms of drug interactions. Nowadays, both human liver specimens and expressed human P450 enzymes are commercially available and it is not difficult to determine a profile of metabolic drug interactions *in vitro*. However, the proper interpretation and quantitative extrapolation of *in vitro* data to *in vivo* situations require a detailed understanding of the overall pharmacokinetics of the drugs involved. Consideration should be given to the site of interaction, the time-courses of the unbound drug concentration at the site, the effects of drug transporters on the pharmacokinetics, and the possible contribution of metabolites to the interaction.[12]

Moreover, the quantitative prediction of drug interactions is difficult because of the following reasons. Firstly, the intestinal CYP3A4 plays a significant role in the first-pass metabolism of orally administered drugs. For example, several human *in vivo* studies have shown that midazolam, felodipine, cyclosporine, and buspirone are extensively metabolized in the intestine.[13] Although Caco-2 cells are used in predicting the extent of intestinal absorption, it is difficult to predict the intestinal metabolism due to the very low expression of CYP3A4 in this cell line.[14] It is also known that CYP3A4 does not distribute uniformly along the length of the intestine: it

is expressed more in the jejunum than in the ileum.[15] In addition, quantitative prediction of oral bioavailability is difficult due to the synergistic role of CYP3A4 and efflux transporters, such as MDR1, in reducing the intestinal absorption of substrate drugs.[16-20] The MDR1 is expressed more in the ileum than in the jejunum.[21] Although the intestine is also considered as an important site of drug interactions, the extent of intestinal metabolism is unpredictable in many cases. Secondly, CYP3A4 recognizes a wide range of substrates and some structural flexibility has been suggested at the substrate recognition site.[22] Consequently, the enzyme kinetics of CYP3A4 is sometimes complicated. Indeed, simple competitive inhibition theory has often failed to explain interactions *via* CYP3A4.[23] Thirdly, a series of CYP3A4 substrates apparently act as mechanism-based inhibitors which covalently bind to the enzyme. For these drugs, the recovery of CYP3A4 activity depends on regeneration of the enzyme at the target site. For this reason, predictions of the mechanism-based interactions from *in vitro* data require more complicated kinetic models compared with reversible inhibitors.[7,8,13,24-26] Considering these complex factors, it is reasonable to conclude that, by using only *in vitro* experimental data, precise prediction of *in vivo* drug interactions is not easy for the variety of drugs that are metabolized by CYP3A4. One of the practical methods to overcome this problem is to use *in vivo* information on interaction data of probe drugs of CYP3A4. This approach would enable the prediction of various drug interactions from results of a small number of drug interaction studies carried out early in the course of drug development.

The objective of the present study is to construct a framework for the prediction of various drug interactions mediated by CYP3A4 using minimum *in vivo* information on drug interactions. We selected midazolam as a standard substrate and ketoconazole or itraconazole as a standard inhibitor. We have aimed to keep the method as simple as possible from a practical viewpoint while, at the same time, remaining theoretically accurate.

METHODS

Literature search

The analysis is based on 113 *in vivo* studies reported in 78 articles published over the period 1983 to 2006 (Tables I and II). Based on information from a comprehensive review[9], we added some new data from the literature. Some substrates and

inhibitors were removed from the original information due to the small contribution or low selectivity for CYP3A4. All studies were used if the report included information on the dosage regime and the increase in AUC. A survey of a series of articles revealed that, in general, inhibitor drugs were administered consecutively for more than several days to attain steady-state conditions and substrate drugs were given as a single dose administration.

Theory

The oral clearance (CL_{oral}) of drugs is given by Eq. 1 where CL_{tot}, CL_h, CL_r, F_a, F_g and F_h are the total body clearance, hepatic clearance, renal clearance, absorption ratio, and the gastrointestinal and hepatic availabilities, respectively. The reason why F_a is located at the left-side in Eq. 1 is that the current analysis (right-side terms) should focus on events after absorption.

$$CL_{oral} \cdot F_a = \frac{CL_{tot}}{F_g \cdot F_h} = \frac{CL_h + CL_r}{F_g \cdot F_h} \qquad \text{Eq. 1}$$

Assuming the well-stirred organ model,[27] Eq. 1 can be converted to Eq. 2 where fu and $CL_{int,h}$ are the unbound fraction of the drug in the blood, and the intrinsic clearance of the liver, respectively. This equation represents a general relationship between the oral clearance and the intrinsic clearance of the liver.

$$CL_{oral} \cdot F_a = \frac{fu \cdot CL_{int,h}}{F_g} + \frac{CL_r}{F_g \cdot F_h} \qquad \text{Eq. 2}$$

In the present study, two simplifications were made with respect to Eq. 2. Firstly, we assumed that CL_r can be ignored, which is frequently the case for lipophilic CYP3A4 substrates. Secondly, we assumed that F_g can be regarded as 1.0 hypothetically. This simplification does not necessarily mean that the gastric metabolism is insignificant. Rather, it means that the gastric metabolism is assumed to occur in proportion to the hepatic metabolism as if it is a part of the liver. This may allow some overestimation of $CL_{int,h}$ as a consequence. Significant gastric first-pass effects are well established facts for some CYP3A4 substrates; Fg values of midazolam, felodipine, cyclosporine and buspirone are reported to be 0.57, 0.45, 0.39 and 0.21, respectively.[13,16] In the future,

it may be advantageous to distinguish between gastric and hepatic metabolism by CYP3A4. At present, however, we have no alternative but to accept this simplification, since we do not know the extent of the *in vivo* gastric metabolism for all of the drugs analyzed in the present study. In this connection, it is worthy of note that incorporation of gut wall CYP3A4 inhibition did not result in a general improvement in drug interaction predictions in a recent report.[28] Overall, Eq. 2 becomes Eq.3 with these simplifications.

$$CL_{oral} \cdot F_a \cong fu \cdot CL_{int,h} \qquad \text{Eq. 3}$$

Then, we considered a relationship between the intrinsic clearance and metabolic drug interactions under an assumption of the rapid equilibrium of the drug concentration between the blood and the hepatocyte. It is often the case that a drug is metabolized by more than two pathways. In Eq.4, we assume two intrinsic metabolic clearances, $CL_{int,3A4}$ and $CL_{int,others}$, which represent the metabolism mediated by CYP3A4 and the sum of other metabolic pathways, respectively.[11,29]

$$CL_{int,h} = CL_{int,3A4} + CL_{int,others} \qquad \text{Eq. 4}$$

In the following equations, asterisks denote parameters altered by a drug interaction. When the metabolism of CYP3A4 is inhibited by a drug interaction, the altered clearance is given by Eq. 5, where I is the unbound concentration of the inhibitor at the interaction site, and K_i is the inhibition constant.

$$CL^{*}_{int,3A4} = \frac{CL_{int,3A4}}{1+\frac{I}{K_i}} \qquad \text{Eq. 5}$$

Equation 5 is applicable to both competitive and non-competitive inhibitions, since the drug concentration *in vivo* is usually much lower than the K_m value.

Here, we define the ratio of the contribution of CYP3A4 to oral clearance (CR_{3A4}) by

$$CR_{3A4} = \frac{CL_{oral} - CL_{oral,-3A4}}{CL_{oral}} \qquad \text{Eq. 6}$$

where $CL_{oral,\text{-}3A4}$ is an altered *in vivo* oral clearance when $CL_{int,3A4}$ is blocked completely. $CL_{oral,\text{-}3A4}$ is given by Eq. 7 based on Eqs. 3 and 4.

$$CL_{oral,\text{-}3A4} \cdot F_a = fu \cdot (CL_{int,h} - CL_{int,3A4}) \qquad \text{Eq. 7}$$

From Eqs. 6 and 7, CR_{3A4} is given by Eq. 8, which indicates that the ratio of the *in vivo* contribution of CYP3A4 to the oral clearance has the same value as the fraction metabolized by CYP3A4 to inhibition (fm_{CYP3A4}), which is determined by examining the effect of CYP3A4 selective inhibitors / antibodies on drug metabolism by human liver microsomes when the urinary excretion is very low and rapid equilibrium is achieved in the liver. These relationships have been widely used for prediction of *in vivo* clearances in the presence of drug interactions or CYP enzyme polymorphisms, as reported by other groups.[11,29]

$$CR_{3A4} = \frac{CL_{int,3A4}}{CL_{int,h}} \qquad \text{Eq. 8}$$

Equation 5 can be converted to Eq. 9 using Eqs. 6 and 8.

$$CL^*_{int,h} = \frac{CR_{3A4} \cdot CL_{int,h}}{1 + \dfrac{I}{K_i}} + (1 - CR_{3A4}) \cdot CL_{int,h}$$

$$= (1 - CR_{3A4} \cdot \frac{I}{I + K_i}) \cdot CL_{int,h} \qquad \text{Eq. 9}$$

To estimate *AUC* from Eq. 9, the equation needs to be integrated with time. For this purpose, the time-averaged apparent inhibition ratio (IR_{3A4}) is defined by Eq. 10.

$$IR_{3A4} = \frac{I_{app}}{I_{app} + K_i} \qquad \text{Eq. 10}$$

where I_{app} is the time-averaged apparent unbound concentration of the inhibitor in the liver. The increase in the ratio of AUC caused by a drug interaction (Eq. 11) is derived from Eqs. 9 and 10. We assumed here that the value of IR_{3A4} for an inhibitor is the same for any substrate.

$$\frac{AUC^{*}_{oral}}{AUC_{oral}} = \frac{CL_{oral} \cdot F_{a}}{CL^{*}_{oral} \cdot F_{a}} = \frac{CL_{int,h}}{CL^{*}_{int,h}} = \frac{1}{1 - CR_{3A4} \cdot \dfrac{I_{app}}{I_{app} + K_{i}}}$$

$$= \frac{1}{1 - CR_{3A4} \cdot IR_{3A4}} \qquad \text{Eq. 11}$$

Eq.11 indicates that an AUC increase by a drug interaction between any oral drug *via* CYP3A4 can be predicted if the CR_{3A4} of the substrate and the IR_{3A4} of the inhibitor are available.

It needs to be mentioned that the above theory may not be applicable directly to mechanism-based inhibitors. However, the final form of Eq. 11 can be accepted even for mechanism-based inhibitors by regarding the IR_{3A4} values as an overall inhibition ratios of CYP3A4 at the equilibrium state between inactivation and generation of the metabolizing enzyme. From this viewpoint, the definition of *IR* by Eq. 10 is invalid for mechanism-based inhibitors.

Calculation of CR_{3A4} and IR_{3A4} values

The values of CR_{3A4} and IR_{3A4} for various substrates and inhibitors were calculated sequentially according to the following steps based on AUC increases in the 53 interaction studies which are indicated by underlines in Table I. (1) We assumed that the CR_{3A4} value of simvastatin is 1.0, since it has been reported that simvastatin is a selective substrate of CYP3A4[30] and a search of the literature showed that the plasma AUC of simvastatin tends to be increased most markedly following inhibition of CYP3A4. It was confirmed that a reduction of the CR_{3A4} value of simvastatin to 0.95 did not affect the overall outcomes of the present analysis. (2) Once we assumed the CR_{3A4} value for simvastatin, the IR_{3A4} value of itraconazole, a typical inhibitor, was obtained based on Eq. 11, using the result of a drug interaction study involving simvastatin and itraconazole. (3) The CR_{3A4} value of midazolam, a typical substrate, was calculated from studies with midazolam and itraconazole using the calculated IR_{3A4} value of itraconazole with Eq. 11. An algebraic mean of the AUC increase was used for the calculation, whenever the results of multiple studies are reported for an interaction set of interest. (4) The IR_{3A4} values of the other inhibitors including ketoconazole, another typical inhibitor, were calculated from interaction studies between the inhibitor and midazolam, using the calculated CR_{3A4} value of midazolam

with Eq. 11. (5) The CR_{3A4} values of other substrates were calculated from interaction studies between the substrate and itraconazole or ketoconazole whenever possible, using the calculated IR_{3A4} value of itraconazole or ketoconazole, respectively, with Eq. 11. (6) For nifedipine, no interaction study with itraconazole or ketoconazole has been reported. Accordingly, the CR_{3A4} value of nifedipine was calculated from the study with nifedipine and diltiazem, using the calculated IR_{3A4} value of diltiazem, with Eq.11. Diltiazem was selected, since the AUC of nifedipine was most significantly increased by the administration of diltiazem.

RESULTS

We surveyed 113 *in vivo* drug-drug interaction studies published in 78 articles shown in Tables I and II. The CR_{3A4} values of 14 substrates and the IR_{3A4} values of 18 inhibitors were calculated using Eq. 11 based on the results of 53 clinical studies (the estimation set), which are indicated by the underlined article numbers in Table I. As shown in Table III, high CR_{3A4} values of more than 95% were calculated for simvastatin, lovastatin, buspiron, and nisoldipine, 85-94% for triazolam, midazolam, felodipine, and 70-84% for cyclosporin, nifedipine, and alprazolam. High IR_{3A4} values of more than 95% were estimated for ketoconazole (daily dose 200-400 mg), voriconazole (400 mg) and itraconazole (100-200 mg), 85-94% for telithromycin (800 mg), clarithromycin (500-1,000 mg), saquinavir (3,600 mg) and nefazodone (400 mg), and 70-84% for erythromycin (1,000-2,000 mg), diltiazem (90-270 mg), and fluconazole (200 mg), and verapamil (240-480mg).

The current method enabled predictions of the AUC increase caused by drug-drug interactions of any combination of the substrates and inhibitors. In order to validate the suitability of the present method, the extent of increase in AUC by drug interaction was predicted for the remaining 60 clinical studies (the validation set), which are indicated by the article numbers without an underline in Table I, and the results were compared with the observed values (Fig. 1B). This prediction was performed by substituting the values of CR_{3A4} and IR_{3A4} shown in Table III and IV, respectively in Eq. 11. As shown in Fig. 1B, with the current method, we could predict the increase in AUC within 67-150% of the observed AUC increase for 50 clinical studies (83%), and within 50-200% for 57 clinical studies (95%).

In the calculation of CR_{3A4} and IR_{3A4} values, the algebraic mean of the increase in